

SAFETY AND PERFORMANCE OF A NEW TYPE OF PHOTOVOLTAIC MODULE INVERTER: LABORATORY AND FIELD TEST RESULTS

*Saiful Islam, Achim Woyte and Ronnie Belmans
Department of Electrical Engineering
Katholieke Universiteit Leuven
Kasteelpark Arenberg 10, B-3001 Leuven, Belgium
Phone (32)16- 321042, Fax (32)16- 32 1985
E-mail: saiful.islam@esat.kuleuven.ac.be*

Keywords: AC module Inverters, Grid-connected systems, Islanding, Photovoltaic power systems, Safety.

ABSTRACT

In the framework of the European research and demonstration project PV2go, a new type of AC module has been developed. In this research work, safety and quality requirements for this AC module have been identified. Its performance has been evaluated for prototype inverters. In laboratory tests carried out at the K.U. Leuven, special concern was given to the subject of unintended islanding. Furthermore, its overall performance has been evaluated. The laboratory tests have to show whether the so-called PV2go inverter can comply with the expectations and where improvements are still necessary. Afterwards, the inverters with the photovoltaic modules (AC modules) have been tested under typical European field condition. Shadowing effects have been considered in the measurements, hence, providing realistic performance data for operation under non-optimum conditions.

1 INTRODUCTION

AC modules are a recent form of grid-connected PV systems. They have brought the well-known and highly acclaimed modularity of PV to the 100 watt-peak level (for grid-connected systems), allowing the installation of literally any size of grid-connected PV systems at almost the same price per watt-peak. This has recently stimulated the creation of new product-market-combinations: 100 to approx. 800 watt-peak systems for direct sale to private people. Because of the small system size the investment is well within reach of many people and the power can be fed directly into the grid without any additional requirements ("plug and play"). This has opened a new and successful market for grid-connected PV systems. Further development of AC-modules (especially the inverter) in terms of performance, reliability, lifetime, size and price is essential to bring the total system price to a level that allows full competition with other sources of electricity. At present, AC-modules are commercially available at system prices ranging from 8 to 14 euro per watt-peak. A further reduction of the price by a factor of 2 is envisaged within the next five years.

As pointed out in the White Paper "Energy for the future" [1] of the European Commission, the main target of photovoltaic R&D projects is a profound cost reduction for solar electricity generation down to 3 Euro/Wp on the mid term. To achieve this goal, a new generation of AC modules needs to be developed, and production volume must be increased to a larger scale.

Under the framework of the European research and demonstration project PV2go, a new type of AC module has been developed. In this research work, safety and quality requirements for this AC module have been identified. Its performance has been evaluated for prototype inverters. In laboratory tests carried out at the K.U. Leuven, special concern was given to the subject of unintended islanding. Furthermore, measurements of the overall performance of the PV2go inverter have been carried out.

Field tests have been carried out according to IEC 61724 [2] at the K.U. Leuven tests facilities for two AC modules. The objective of the field test is to evaluate the performance of the AC-module under actual meteorological conditions. Module voltage and current, inverter output power as well as meteorological parameters are logged using a modular data acquisition system [3]. Shadowing effects have been considered in the measurements, hence, providing realistic performance data for operation under non-optimum conditions.

2 ISLANDING TESTS

2.1 Technical Background

As every decentralized production unit connected to the public grid, PV inverters have to comply with common safety standards. A major issue is to avoid non-intentional islanding with the grid being disconnected at fault conditions or for maintenance purposes.

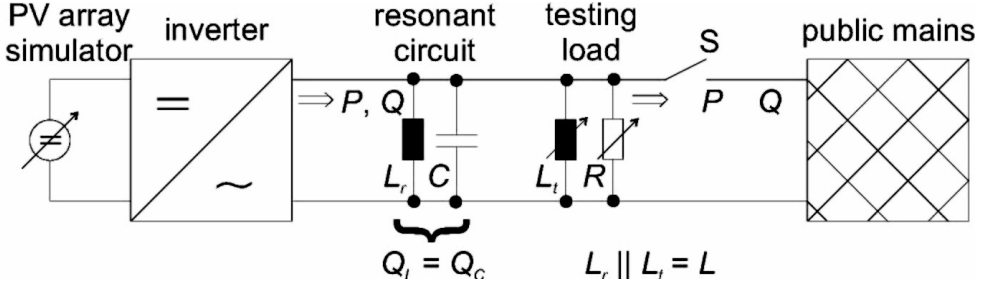


Figure 1: Test circuit for islanding protection [4]

For testing the islanding behaviour of a PV inverter, a generally applicable test circuit is available (figure 1). Parameters for the test circuit vary from country to country, especially with regard to the operating points to be tested and to the size of the resonance circuit.

In principle, every self-commutated inverter is able to operate in islanding mode [5]. If no particular control algorithm for islanding prevention is applied, the load conditions under which islanding occurs depend only on the inverter's frequency and voltage limits. Assuming constant active and reactive output power before and after grid disconnection, the power balance leads to voltage and frequency in islanding operation is implied by the following equations.

$$\frac{\Delta P}{P} = 1 - \frac{U_{grid}^2}{U_{island}^2} \quad (1)$$

$$\frac{\omega_{island}}{\omega_{grid}} \cdot \frac{\Delta P}{P} - \frac{\Delta Q}{Q} = \left(\frac{\omega_{island}^2}{\omega_{grid}^2} - 1 \right) \cdot \frac{Q_c}{Q} + \frac{\omega_{island}}{\omega_{grid}} - 1 \quad (2)$$

In these equations P and Q indicate the inverter's operating point. Q_c is the reactive power supplied by the resonance circuit's capacitor. ΔP and ΔQ are active and inductive reactive power supplied to the grid before grid disconnection. They can be adjusted by tuning the test load. For a given capacity and inverter power, it is possible to determine a so-called non-detection zone (NDZ) in the ΔP - ΔQ -domain where an inverter with predefined voltage and frequency limits will operate in

islanding mode [6]. In figure 2 the NDZs of a 200 W inverter are indicated for different combinations of P , Q and Q_C .

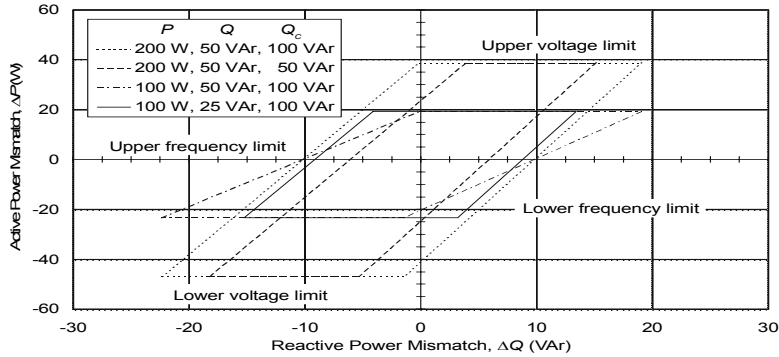


Figure 2: Calculated non-detection zones of a 200 W inverter at different power levels and for different load capacities with fixed voltage and frequency limits

In most islanding test specifications existing worldwide, Q_C must be constant at 100 VAr disregarding the operating point of the inverter [7]. In islanding test specifications as they are applied in the UK and the USA, Q_C is variable. The parameter determining the size of the resonant circuit is not reactive power Q_C or Q_L , but the quality factor Q_r (3) of the resonance circuit,

$$Q_r = \frac{Q_C}{P} \quad (3)$$

In the USA the quality factor must be 2.5 and in the UK it must be higher than 0.5.

2.2 Measurements and Results

The test circuit from figure 1 has been set up in the laboratory. The precise experimental set-up is described in [8] including a detailed description of the applied PV array simulator. The steady-state current-voltage curve of the PV simulator has been recorded for two significant operating points (figure 3). The irregular fluctuations of the curves in figure 3 are not the characteristics of the PV simulator but are caused by the inertia of the x-y-plotter.

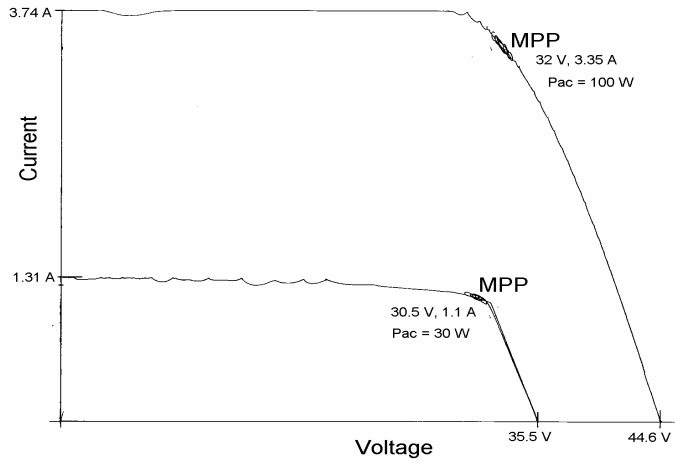


Figure 3: Current-voltage curves of the PV simulator and trajectory of the PV simulator loaded with the PV2go inverter for two operation points corresponding to 30 W and 100 W AC power

The PV2go inverter has the following technical specifications indicated in Table 1:
Table 1: Technical Specifications of the PV2go Inverter

	P [W]	Q_{out} at P_r [VAr]	Relay settings			
			U_{min} [V]	U_{max} [V]	f_{min} [Hz]	f_{max} [Hz]
$P=P_r$	100	10.1	207	253	49.8	50.2
$P=0.3P_r$	30	11.6				

The NDZ has been recorded for the operating conditions indicated in Table 2.

Table 2: Operating Points and Size of the Resonant Circuits as well as Corresponding Quality Factors for the Tests Carried Out with the PV2go-Inverter ($P_r = 100$ W)

	$Q_C = 50/15$ VAr	$Q_C = 100$ VAr	$Q_C = 250/75$ VAr
30 % of P_r	$Q_r = 0.5$	$Q_r = 3.33$	$Q_r = 2.5$
100 % of P_r	$Q_r = 0.5$	$Q_r = 1$	$Q_r = 2.5$

The NDZs have been recorded at 30 % and 100% rated power for different values of Q_C or Q_r by applying the test circuit from figure 1. Samples have been taken by stepping through the ΔP - ΔQ -domain in steps of 5 % of the inverter's rated power. In most European countries, an inverter under worst-case conditions must switch

off within 5 s after grid disconnection. Hence, the inverter is accounted for being in islanding operation if it does not switch off within 5 s after switch S has been opened. For each point $(\Delta P, \Delta Q)$ at least four tests have been carried out. If these showed varying results, three more tests were added. A point is located within the NDZ if islanding occurred at least twice.

Additionally, in order to examine the influence of the under- and over-frequency relay settings, the NDZs have been recorded for $Q_C = 100 \text{ VAr}$ with a second inverter with frequency limits adjusted to 49 Hz / 51 Hz (figure 4).

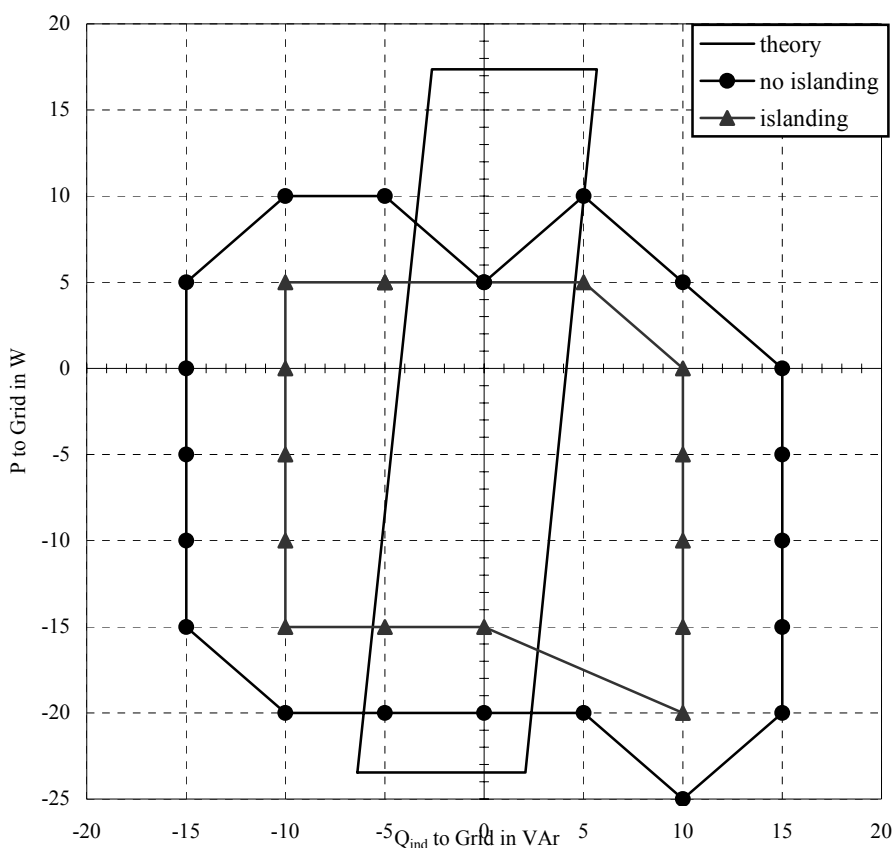


Figure 4: Non-detection zone, $P = P_r$, $Q_C = 100 \text{ VAr}$ ($Q_r = 1$), $\text{NDZ} = 350 \text{ W} \cdot \text{VAr}$

In the recorded NDZ diagrams (figures 4 to 8), sampling points where the inverter was operating in islanding mode are identified by a triangle. Sampling points where no islanding occurred are identified by a circle and the NDZ derived from (1) and (2) is bounded by a solid black line.

As figures 4 to 8 shows, the sizes of the NDZ generally correspond to the theoretical NDZ, indicating the proper functioning of the inverter power control algorithms and of its frequency and voltage relay settings. Generally, the results correspond well to those from previous measurements with different other module inverters [9]. Islanding occurred in figure 6 and figure 8 just outside the theoretical NDZs with a small reactive power mismatch of several VAR. These variations are due to slight variations in the supply network. The sizes of the NDZ indicate that voltage and frequency monitoring function properly. According to the design specifications additional islanding prevention methods have not been implemented.

Without parallel capacitance in the test circuit no islanding occurs. However, as soon as a parallel capacitance is applied, there are significant NDZ's especially for high power. The NDZ's are rather narrow in the ΔQ direction, but large in ΔP direction. This is because the frequency relay could be set rather narrow, while the voltage relay setting always has to consider the wider variability of the grid voltage in the field.

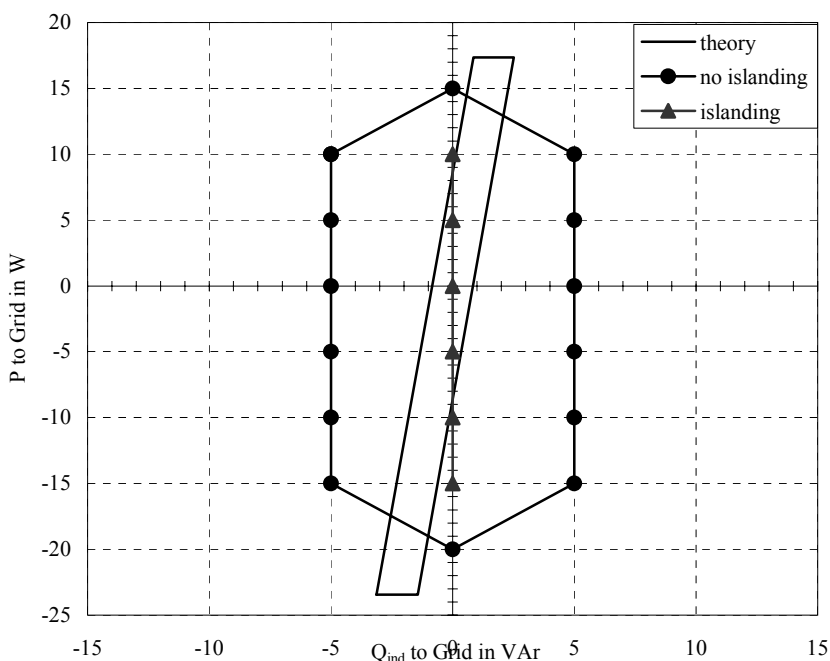


Figure 5: Non-detection zone, $P = P_r$, $Q_C = 100 \text{ VAR}$ ($Q_r = 1$), $\text{NDZ} = 150 \text{ W} \cdot \text{VAR}$

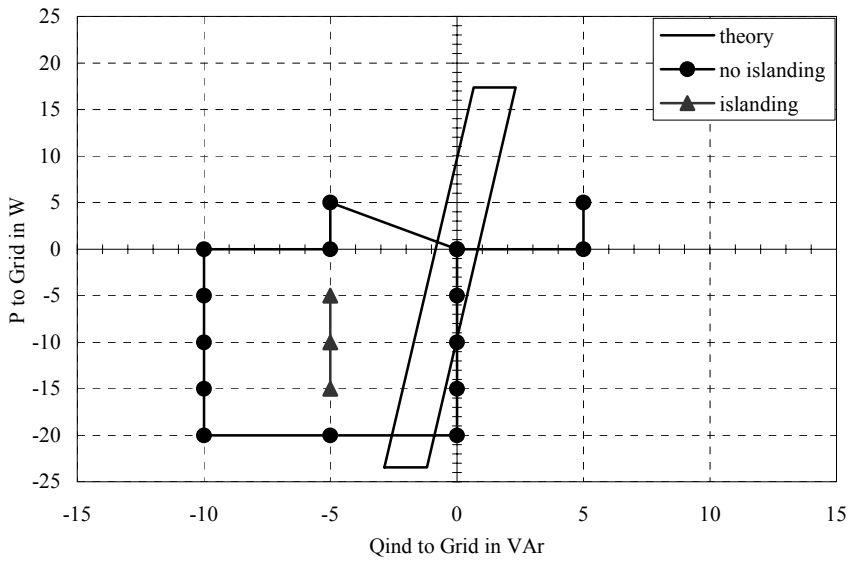


Figure 6: Non-detection zone, $P = P_r$, $Q_C = 100 \text{ VAR}$ ($Q_r = 1$), $NDZ = 75 \text{ W} \cdot \text{VAR}$

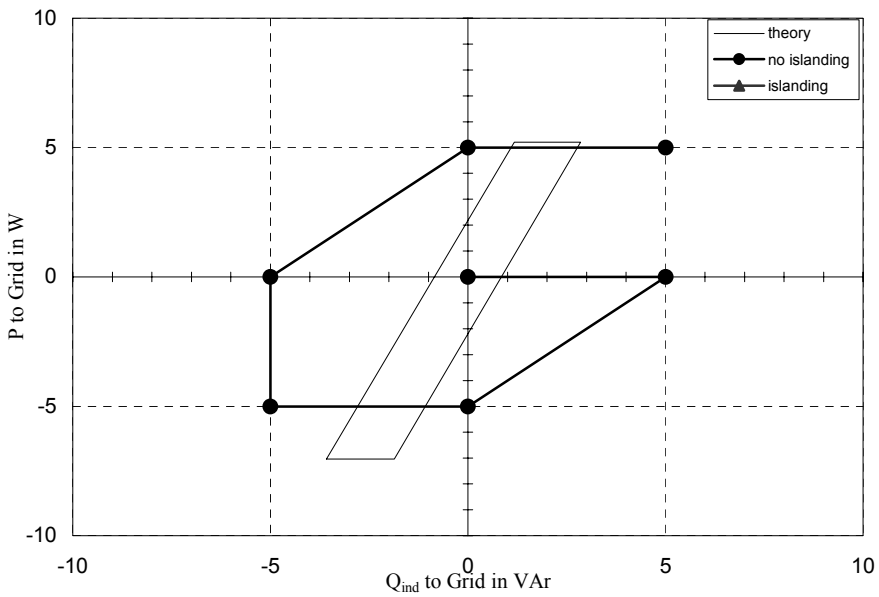


Figure 7: Non-detection zone, $P = 0.3 P_r$, $Q_C = 100 \text{ VAR}$ ($Q_r = 3.33$), $NDZ = 0 \text{ W} \cdot \text{Var}$

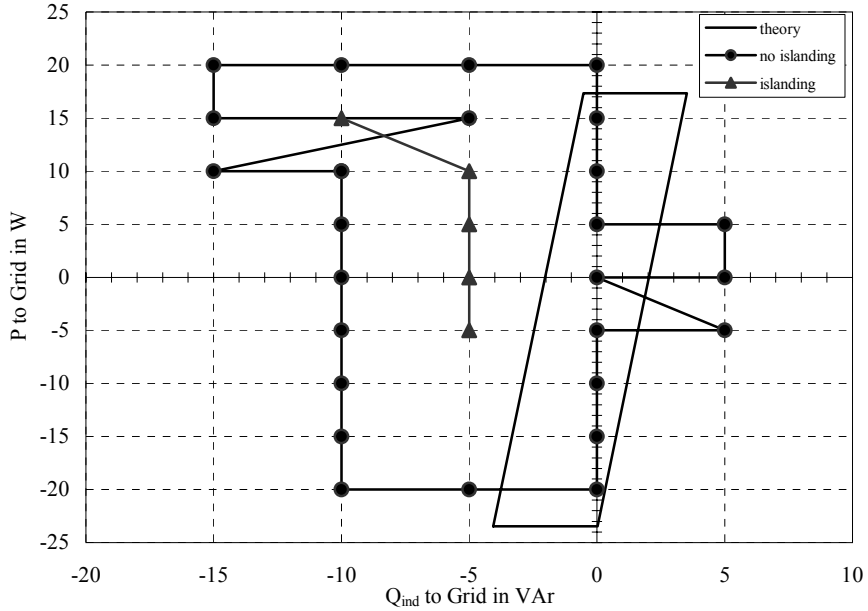


Figure 8: Non-detection zone, $P = P_r$, $Q_C = 250 \text{ VAr}$, ($Q_r=2.5$), $\text{NDZ}=175\text{W}\cdot\text{VAr}$

From the number of points where islanding occurred and the discretisation of 5 W per step, the size of the NDZ can be calculated for the different operating points (Table 3). The results in Table 3 indicate that the inverter would not be accepted by the distribution network operator in any of the countries where a type approval with a resonant circuit is applied. In order to be in accordance with the different grid connection guidelines, an external interface would have to be applied.

Table 3: Size of Non-detection Zones for Different Operating Points ($P_r = 100 \text{ W}$)

	$Q_C = 50/15 \text{ VAr}$	$Q_C = 100 \text{ VAr}$	$Q_C = 250/75 \text{ VAr}$
30 % of P_r	0 W·VAr	0 W·VAr	0 W·VAr
100 % of P_r	25 W·VAr	75 W·VAr	175 W·VAr

2.3 Islanding Prevention Techniques

Implementing additional anti-islanding measures is beyond the scope of this research work. However, a wide variety of islanding prevention methods for grid-connected PV systems has been proposed in literature [5,10-12]. Most methods work well for a large number of load cases but when tested by applying a particular worst-case test circuit in order to simulate the power island in the laboratory, some

special load cases can always be identified under which the particular method fails to detect the power island [5,9,10-13].

A number of additional islanding prevention methods have been documented. Generally, two approaches for implementing islanding prevention in connection with the inverter can be identified. One of them is to supervise a third criterion that can indicate abnormal operating conditions being independent of voltage and frequency. Monitoring of phase jumps or harmonics is such an approach as is monitoring of the grid impedance by current pulse injection [14-16]. Another approach is to design an unstable current and phase controller. Here it is the intention to make voltage or frequency relays in an isolated grid section trip, even when generation and load are matched. This is obtained by positive feedback of a possible voltage, frequency, or phase bias, causing the current and phase control circuits to become unstable when the mains are disconnected [10,17].

3 EFFICIENCY AND POWER QUALITY MEASUREMENTS

Efficiency and power quality parameters have been measured for a number of indicative operating points (Table 4).

Table 4: Operating Points and Measured Performance Data for the PV2go-Inverter ($P_r = 100$)

<i>Op. Point</i> [W]	<i>AC Power</i> [W]	<i>Eff.</i> [%]	<i>PF [-]</i>	<i>Cos φ</i> [-]	<i>THD (U)</i> [%]	<i>THD (I)</i> [%]
5	5.697	82.34	0.42	0.43	2.5	15.1
8	7.467	85.03	0.52	0.53	2.6	14.6
10	10.931	87.62	0.66	0.68	2.6	12.8
15	15.719	89.81	0.79	0.81	2.6	10.9
20	19.82	90.92	0.86	0.87	2.4	9.5
30	29.34	91.77	0.93	0.94	2.9	6.3
40	39.72	92.31	0.96	0.97	2.6	6.3
50	49.55	92.32	0.97	0.98	2.6	5.5
60	59.95	92.55	0.98	0.99	2.6	5.6
80	79	92.44	0.98	0.99	2.4	4.4
100	100	92.30	0.99	0.99	2.5	4.9
110	109.92	92.13	0.99	0.99	2.6	4.9

With the data from Table 4 the European efficiency has been calculated according to (4).

$$\eta_{EU} = 0.03\eta_{5\%} + 0.06\eta_{10\%} + 0.13\eta_{20\%} + 0.10\eta_{30\%} + 0.48\eta_{50\%} + 0.20\eta_{100\%} \quad (4)$$

The indexed η_{EU} values indicate the inverter efficiency at the given percentage of rated AC power [18]. The European efficiency calculated with (4) is 91.50%.

Current harmonics at 10 and 30 % of rated power are not limited by standards. However, the current harmonics at these levels are normalized to the current fundamental of the full system output. Comparing them to the limits from IEEE 929:2000 [19] that have to be applied for 100% of rated power, shows that results are well within the limits. Harmonic spectra of inverter output currents at 10 and 30 % as well as 100% of rated power normalized on current fundamental of AC power are also compared to the limit values according to IEEE 929:2000.

All measurements including the harmonic analysis have been carried out with a *Voltech PM 3000 A Universal Power Analyzer*. For acquisition of the measurements an average of 64 samples has been chosen in order to filter the low-

frequent fluctuations introduced by the MPP tracker. The results are shown in figures 9 to 13.

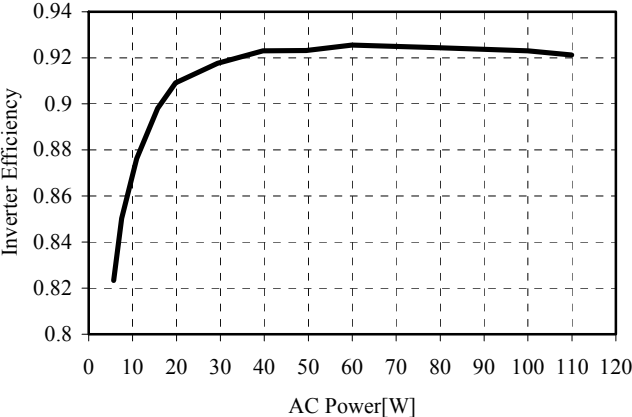


Figure 9: Conversion efficiency as a function of AC power

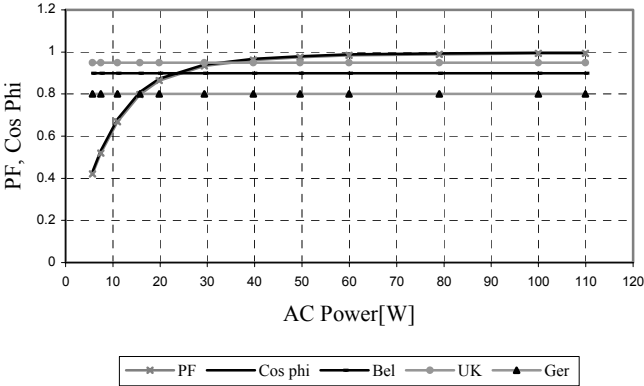


Figure 10: Cos φ and power factor as a function of AC power and limits from different DNO guidelines

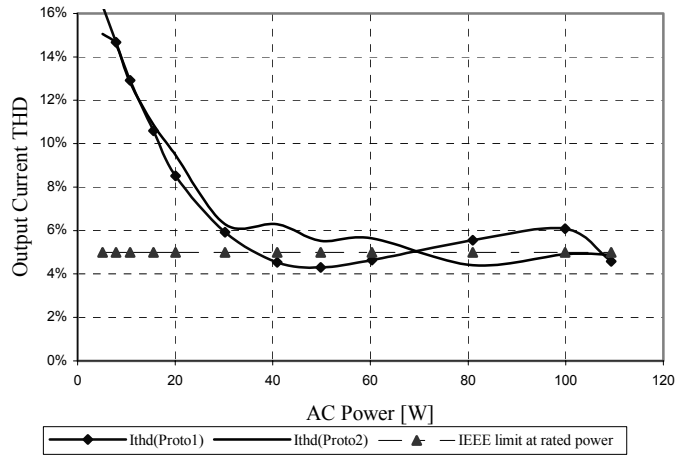


Figure 11: Current THD as a function of AC power and limit value according to IEEE 929:2000

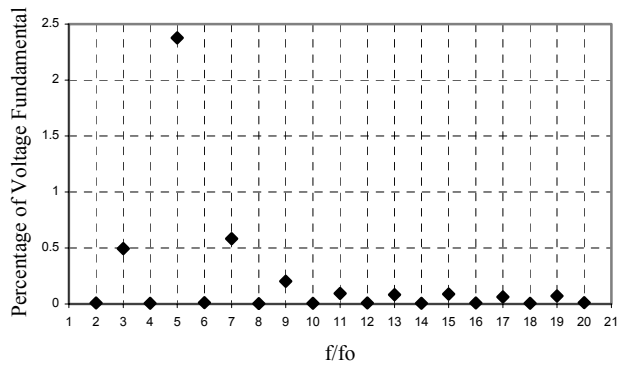


Figure 12: Harmonic spectrum of the grid voltage in percent; voltage fundamental 230 V

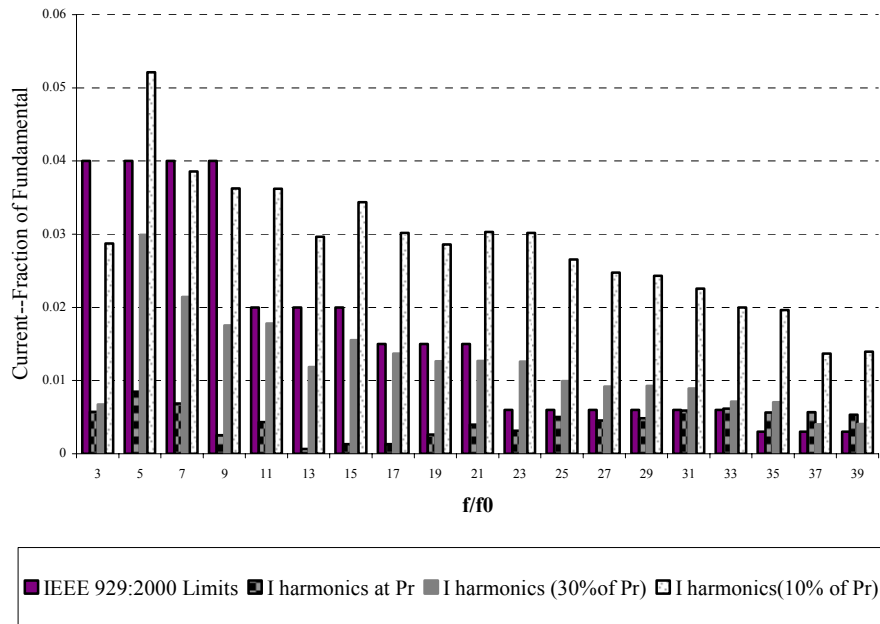


Figure 13: Harmonic spectrum of inverter output currents, normalized on current fundamental of AC power and limit values according to IEEE 929:2000; $I_1(10\%) = 70 \text{ mA}$, $I_1(30\%) = 178 \text{ mA}$, $I_1(100\%) = 435 \text{ mA}$

4 FIELD TESTS

At the K.U. Leuven test site, the two PV2go AC modules (PV2go 1 and PV2go 2 both with PV2go inverter) have been under field test. AC modules and monitoring work are trouble-free since 1 July 2002.

The quantities monitored, are shown in Table 5. Since the test site is partially shadowed by surrounding vegetation, the in-plane irradiance is measured once at a shadow-free position and two more times at positions on the upper and lower edge of the two AC modules.

Table 5: Monitored Quantities and Applied Sensors

<i>Quantity</i>	<i>Symbol / Dimension</i>	<i>N</i>	<i>Sensor</i>
<i>Meteorology:</i>			
Irradiance, global horizontal	$G_h / \text{W}/\text{m}^2$	1	Pyranometer, WMO class II: Kipp & Zonen CM11
Irradiance, diffuse horizontal	$D_h / \text{W}/\text{m}^2$	1	Pyranometer, WMO class II: Kipp & Zonen CM11 with shadow ring CM121
Irradiance, global in-plane	$G_{30^\circ} / \text{W}/\text{m}^2$	3	Silicon reference cells, temperature compensated: 1 per AC module and 1 shadow-free Mencke & Tegtmeyer Si-420 TC
Ambient temperature	$T_{\text{am}} / ^\circ\text{C}$	1	Pt 100 thermo resistance, radiation shielded
<i>AC modules:</i>			
DC module current	$I_{A, \text{Str.}} / \text{A}$	2	Hall effect current transducer: LEM LA 55-P/SP1, 12 windings
DC module voltage	V_A / V	2	Hall effect voltage transducer: LEM LV 100-TENSION, 100V
Module temperature	$T_M / ^\circ\text{C}$	1	Pt 100 thermo resistance back of PV cell
<i>Inverter Outputs:</i>			
AC power from inverter	P_{AC} / W	2	True RMS AC single phase power transducers: Multitek M100 WA1

The data listed in Table 5 are monitored by a *Gantner IDL 100* data logger. The sampling interval is set to one second, while storing measured data as five-minute average values in the logger's RAM. These data are downloaded automatically by a PC once per day and stored for further evaluation. The interface between data logger and PC is implemented as a standard serial RS232 connection. The output signals coming from the sensors are transferred via current loops with 4 to 20 mA in order to achieve an interference-free transmission and a high reliability of the measured data.

The modules under test are shown in figure 14. Actual module powers have been given in Table 6. The upper module on figure 14 is called PV2go1, the lower one PV2go2. PV2go2 is slightly more shadowed than PV2go1, which explains the slightly lower yield in figures 15 and 16.

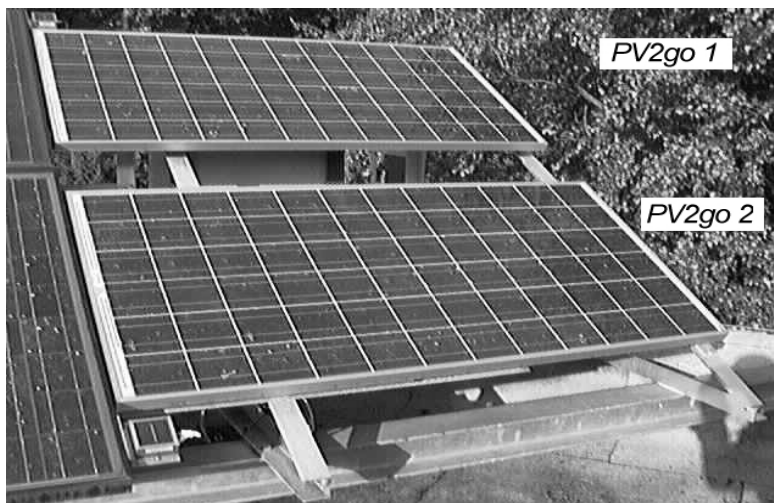


Figure 14: PV2go AC modules on the field test site at K.U. Leuven; on the left at the lower and upper module frame see silicon reference cells

Table 6: Applied AC Modules with Inverter PV2go Proto 2; "Location" Refers to Figure 14

<i>Name</i>	<i>Location</i>	<i>Actual Peak Power</i>
PV2go1	up	127.7Wp
PV2go2	down	126.3Wp

For the calculation of shadow losses, the in-plane irradiance on the two AC modules has been linearly interpolated from the measurements of the two reference cells visible in figure 14. For the last two months, the shadow losses had to be calculated on the base of the upper reference cell only, due to failure of the lower of the two reference cells in early June 2003.

Figure 15 shows the yield and losses of both modules on a monthly basis. As a basis for the yield calculations, the actual peak power of the modules as it is indicated in Table 6 has been applied. Figure 16 shows the same data normalized on the reference yield before shadowing, thus indicating the system performance being independent of the solar irradiation at the particular months. Final yield

normalized to reference values as indicated in figure 16 is equal to the monthly performance ratio.

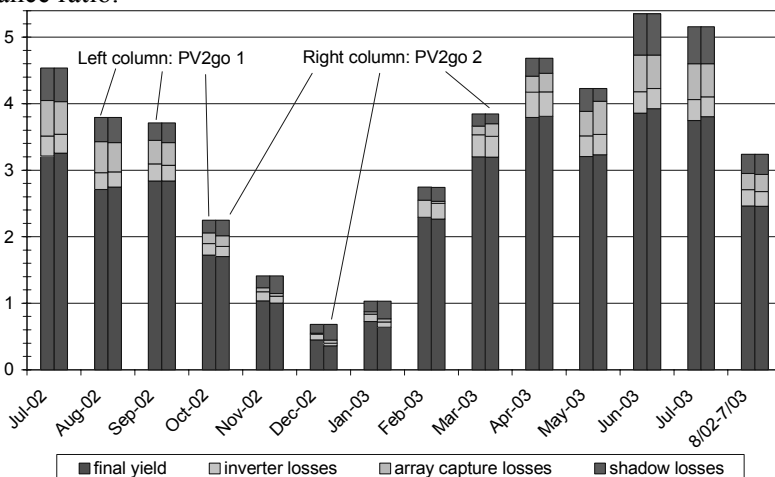


Figure 15: Comparison of daily yield and losses for the two AC modules throughout the year

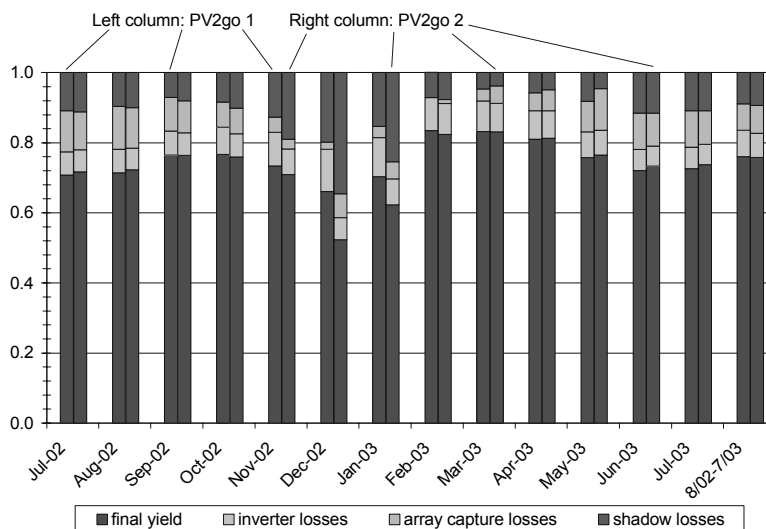


Figure 16: Comparison of daily yield and losses for the two AC modules after normalization on reference yield throughout the year

Throughout the year the module PV2go2 being the lower one of the two, has the higher shadow losses. In the winter month when the solar elevation is very low, this difference becomes especially significant. On an annual basis, the performance ratio of 0.76 for both AC modules is very high; regarding that 9 % of the reference yield during the test year is lost as a consequence of shadowing.

Array capture losses are low in winter due to the lower module temperature. The very low array capture losses from November to February originate from low module temperature (figures 17 and 18) but also indicate that the MPP tracking of the module inverters works well. This is even the case for very low irradiance values, however, extreme partial shadowing as it occurs in December especially to the lower module PV2go 2 leads to increased mismatch losses in comparison to PV2go 1. This is mainly due to current limiting by partial shadowing of a few cells within a sub-string being paralleled by one bypass diode [20].

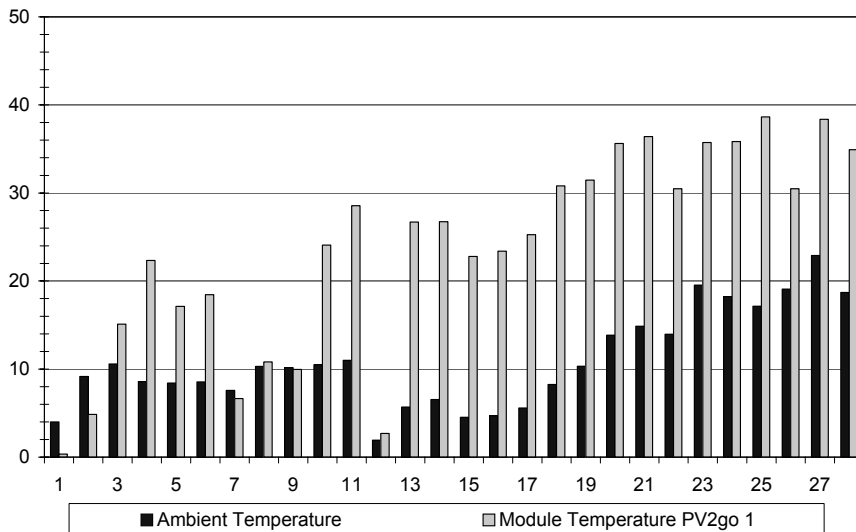


Figure 17: Daily maximum of ambient temperature and PV cell temperature in February 2003

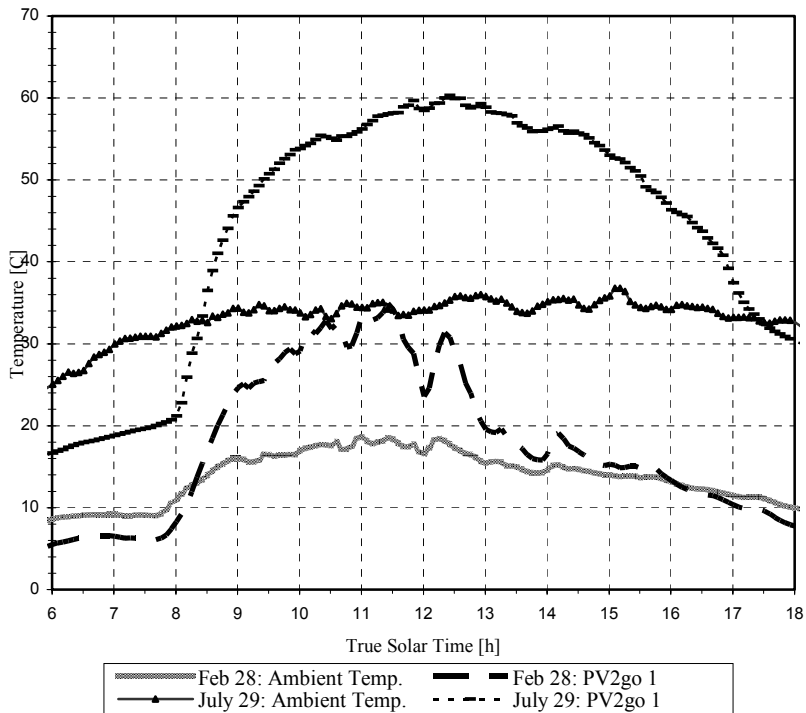


Figure 18: Ambient temperature and PV cell temperature for a summer and a winter day (July 29, 2002 and Feb. 28, 2003)

The inverter losses are comparable for both AC modules. Again, in winter when PV2go2 suffers from much higher shadowing and related array capture losses, this inverter works at lower power more frequently than PV2go1. This generally leads to lower losses in terms of yield but higher losses if normalized to reference yield indicating a lower efficiency while the inverter operates at partial load.

Figure 19 gives the example of a winter day for irradiance an output power of the two AC modules. In the morning there are clear sky conditions while starting around noon the sky becomes more and more overcast. In the late afternoon the sky is fully covered by clouds. During the whole day the AC modules' output powers follow rather exactly the shape of the solar in-plane irradiance indicating proper performance of both AC modules for different characteristic sky conditions.

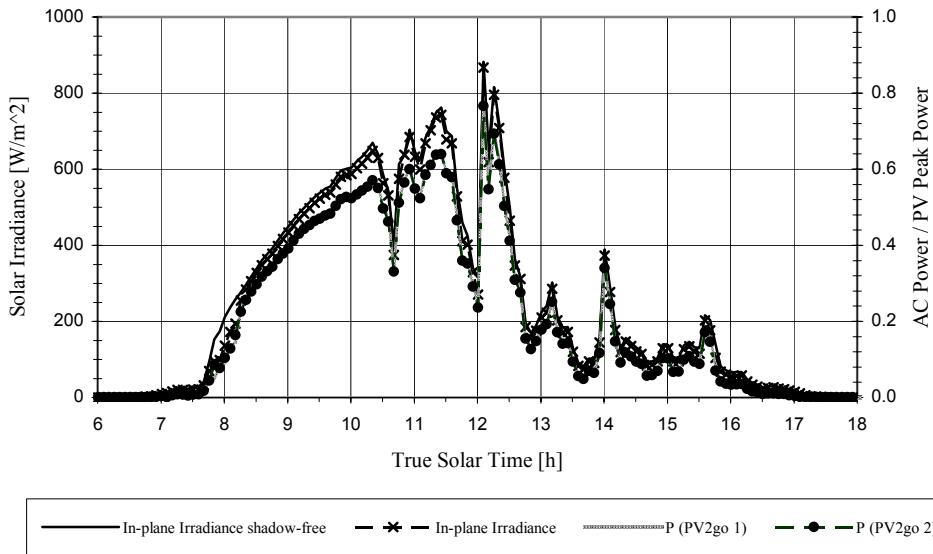


Figure 19: Solar in-plane irradiance (shadowed and shadow-free) and normalized AC power output for two AC modules on a winter day (28/02/2003)

For the same day efficiency has been calculated from five-minute average values of power (figure 20). This efficiency curve measured in the field is very well comparable to the one that measured in the laboratory, indicating a good performance of the PV2go inverter also in the field.

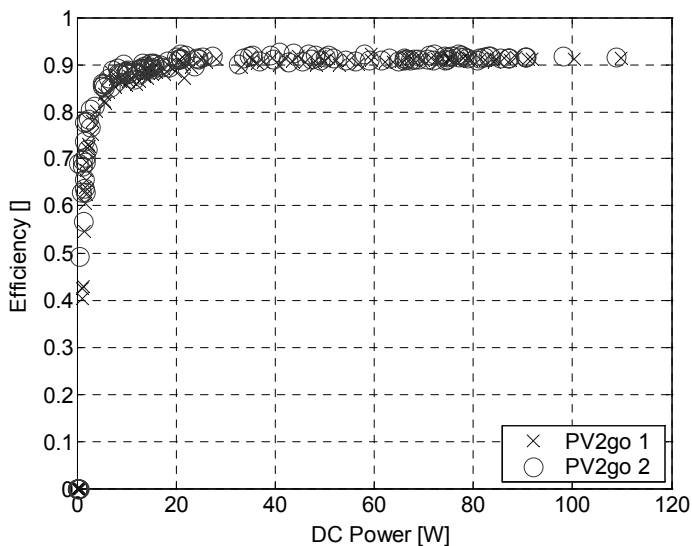


Figure 20: Efficiency values as a function of DC power, based on five-minute average values (28 February 2003)

5 CONCLUSIONS

The PV2go AC module inverter has thoroughly been tested with regard to islanding and other parameters of performance and power quality. In addition the performance of the new inverter has been assessed in the field.

In the initial design phase it was decided not to implement any additional anti-islanding functions in the inverter in order to keep the design simple and inexpensive. This is why, as to be expected from theory, a non-detection zone exists with quality factors of 0.5 and higher. In cases where islanding protection is required, an external grid interface with protection functions as commercially available could be applied.

The non-detection zone has been recorded for different load conditions as required by different national and international standards. At low power, islanding did not occur. At high power, islanding occurred for all relevant load conditions. The non-detection zones recorded correspond with those to be expected from theoretical considerations. This means that the implemented current controller as well as voltage and frequency monitoring function properly.

The total harmonic distortion (THD) as well as the magnitude of all higher-order harmonics is within the limits of international standards, including the strict US standard IEEE 929:2000.

The European efficiency measured in the laboratory is 91.50% with the maximum efficiency being 92.3% for a wide power range.

From the field tests, it can be concluded that the PV2go AC modules, perform well under actual operating conditions in a moderate maritime climate. During the entire field test period, there has been no failure of the AC modules. Although the modules are partly shadowed no increased over-proportional losses are observed as they could occur under severe shadowing due to insufficient MPP tracking. The inverter efficiency in the field equals the laboratory efficiency from 91 up to 93 %.

6 REFERENCES

- [1] European Commission, 1997, "Energy for the Future: Renewable Sources of Energy", White Paper for a Community Strategy and Action Plan, COM (97) 599; Available: <http://europa.eu.int/comm/energy/en/com599.htm>
- [2] "Photovoltaic system performance monitoring – Guidelines for measurement, data exchange and analysis," IEC 61724, November 1998.
- [3] A Woyte, J Nijs, and R Belmans, "Partial Shadowing of Photovoltaic Arrays with Different System Configurations: Literature Review and Field Test Results", *Solar Energy*, **74 (3)**, pp. 217-233, 2003.

- [4] H. Häberlin, and J. Graf, "Islanding of Grid-Connected PV Inverters: Test Circuits and some Test Results," 2nd World Conference and Exhibition on Photovoltaic Solar Energy Conversion, Vienna, Austria, 1998, pp. 2020-2023
- [5] M.E. Ropp, M. Begovic, and A. Rohatgi, "Prevention of Islanding in Grid-connected Photovoltaic Systems," *Progress in Photovoltaics: Research and Applications*, **7(1)**, pp. 39–59, 1999.
- [6] A. Woyte, K. De Brabandere, D. Van Dommelen, R. Belmans, and J. Nijs, "International Harmonization of Grid Connection Guidelines: Adequate Requirements for the Prevention of Unintended Islanding," *Progress in Photovoltaics: Research and Applications*, Vol. 11, No. 6, pp. 407-424, 2003.
- [7] C. Panhuber, "PV System Installation and Grid Interconnection Guidelines in Selected IEA Countries," Report IEA-PVPS T5-04: 2002, 2001.
- [8] A. Woyte, R. Reekmans, and R. Belmans, "Technical Documentation: Islanding Tests of Photovoltaic Inverters", K.U.Leuven, 2000.
- [9] A. Woyte, R. Belmans, and J. Nijs, "Testing the Islanding Protection Function of Photovoltaic Inverters," *IEEE Transactions on Energy Conversion*, **18(1)**, pp. 157-162, 2003.
- [10] J. Stevens, R. Bonn, J. Ginn, S. Gonzalez, and G. Kern, "Development and testing of an approach to anti-islanding in utility-interconnected photovoltaic systems," SAND 2000-1939, Sandia National Laboratories: Albuquerque, 2000.
- [11] C. Panhuber, "Islanding prevention methods," International IEA Workshop on Existing and Future Rules and Safety Guidelines for Grid Interconnection of Photovoltaic Systems, IEA-PVPS Task V Workshop, Zürich, pp. 83–88, 1997.
- [12] W. Bower, and M. Ropp, "Evaluation of islanding detection methods for photovoltaic utility-interactive power systems," Report IEA-PVPS T5-09: 2002.
- [13] RM. Hudson, T. Thorne, F. Mekanik, MR. Behnke, S. Gonzalez, and J. Ginn, "Implementation and testing of anti-islanding algorithms for IEEE 929-2000 compliance of single phase photovoltaic inverters," 29th IEEE Photovoltaic Specialists Conference, New Orleans, 2002, pp. 1414–1419.
- [14] S-J. Huang, and F-S. Pai, "A new approach to islanding detection of dispersed generators with self-commutated static power converters," *IEEE Transactions on Energy Conversion*, **15(2)**, pp. 500–507, 2000.
- [15] GA. Kern, "Sunsine300, utility interactive ac module anti-islanding test results," 26th IEEE Photovoltaic Specialists Conference, Anaheim, 1997, pp. 1265–1268.
- [16] O. Tsukamoto, and K. Yamagishi, "Detection of islanding of multiple dispersed photovoltaic power systems," *Solar Energy*, **58(1)**, pp. 9–15, 1996.
- [17] ME. Ropp, M. Begovic, and A. Rohatgi, "Analysis and performance assessment of the active frequency drift method of islanding prevention," *IEEE Transactions on Energy Conversion*, **14(3)**, pp. 810–816, 1999.

- [18] H. Häberlin,, C. Liebi, and C. Beutler, "Inverters for Grid Connected PV Systems: Test Results of some New Inverters and Latest Reliability Data of the Most Popular Inverters in Switzerland,," 14th European Photovoltaic Solar Energy Conference, Barcelona, 1997, pp. 2184-2187.
- [19] "Recommended Practice for Utility Interface of Photovoltaic (PV) Systems," IEEE Std. 929, 2000.
- [20] A.M. Kovach, "Effect of Partial Shading on the Energy Performance of Photovoltaic Arrays Integrated onto Buildings," PhD thesis, VDI-Verlag, Düsseldorf, Germany.